Resonance and Friction Compensations in a Micro Hard Drive

Wilaiporn Ngernbaht, Kongpol Areerak, Sarawut Sujitjorn*
School of Electrical Engineering, Institute of Engineering
Suranaree University of Technology
Nakhon Ratchasima, Thailand, 30000
*corresponding author: sarawut@sut.ac.th
http://www.sut.ac.th/engineering/electrical/carg/

Abstract: - This paper presents dynamic compensations in a micro hard drive. It reviews dynamic models of the drive in low-and high-frequency regions. The nonlinear friction compensation for low-frequency dynamic is achieved via a fuzzy logic controller. Forward and backward micro-step motion of the read/write head can be nicely performed. Resonance compensation for high-frequency dynamic is achieved via linear compensation. The paper presents some comparison studies of using a cascaded lead compensator, a complex lead-lag compensator, and a searched polynomial compensator. The compensated system's performance is enhanced further by stable nonlinear control. Detailed descriptions of modelling, design, simulation results, and analysis can be found in the paper.

Key-Words: - Resonance, Friction, Compensation, Adaptive tabu search, Fuzzy logic, Hard drive.

1. Introduction

High speed data accessibility is a very demanding specification for today's hard drives. It can be achieved by using effective control technology. Proper servo systems for a hard drive require two controllers namely track-seeking, and track-following controllers, respectively. The control systems are usually subjected to repeatable and nonrepeatable runouts, which need appropriate compensations [1-3]. A high-frequency bandwidth specification is also imposed on a current servo system of a hard drive. Due to drive's imperfection, a hard drive is not rigid and contains many flexible modes that raise vibrations. The resonance modes severely degrade the hard drive performance, and are the causes of the nonrepeatable runout. Hence, resonance modes must be treated properly by compensation in high frequency. Regarding this, the voice-coil-motor (VCM) actuator can be accurately modeled by a transfer function of various resonance modes as in the equation (1) [4, 9]

$$G(s) = \frac{K_T}{Js^2}\prod_{k=1}^{m}\frac{\omega_{nk}{}^2}{s^2 + 2\zeta_k\omega_{nk}s + \omega_{nk}{}^2} \qquad (1)$$

where K_T = torque constant, J = inertia, ζ_k = damping ratio and ω_{nk} = natural frequency of the k^{th} resonance mode. In a micro hard drive, the effects of nonlinear friction in the pivot bearing and the data flex in the VCM become even more pronounced. Even though the VCM used as a read/write head has a high-frequency bandwidth, the data flex connected to it does not. The data flex behaves like a nonlinear damper during its expansion and contraction phases. These movement phases always occur when the read/write head moves away from or back to its home position. Moreover, the friction from the pivot bearing, and the data flex causes severe errors in track following movement of the head. Thus, the low-frequency dynamic of the read/write head is influenced by the nonlinear friction and characteristics caused by the data flex and the pivot bearing. If such nonlinearities were not compensated properly, a great deal of errors in data retrieval due to the head being misplaced would occur. Fig. 1 shows the mechanical structures of a hard drive. Chen et. al. [5] addressed these problems with their proposed composite nonlinear feedback (CNF) control.

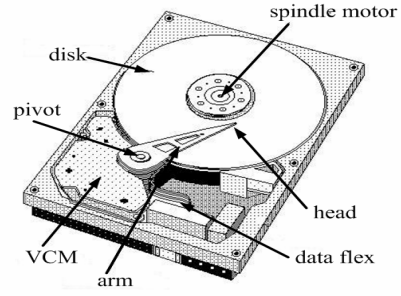

Fig.1 Mechanical structures of a hard drive.

Intelligent control is also an alternative for the servo problems of a hard drive such as use of fuzzy logic [6, 7], etc. Recently, an effective use of resonant filter has been proposed for track-following control [8]; a combined use of reference generator and nonlinear feedback controller has been proposed for track-seeking control [9]; a point-to-point motion control algorithm has been applied for short stroke servo control in a hard drive [10]; Wang and Du et. al. [11, 12] have successfully applied the sliding mode and the nonlinear tracking control approaches to accomplish non-overshoot servomechanisms of hard drives. Extremum seeking control for a hard drive can also be achieved by using intelligent search, e.g. genetic algorithm [13], etc. The reviews of these literatures, even though not exhaustive, give us useful information on modelling of hard drives as well as rooms available for testing some new ideas on linear, nonlinear and intelligent control approaches to the servo problems of hard drives.

In this paper, the authors demonstrate the design of a mixed type of controllers using rule-based and fuzzy logic to treat the effects of nonlinear friction. A few production rules have been added in order to handle the sub-transient dynamic of the head. The overall structure of the controller is very simple and like a switched-type controller. Two or more controllers, each of which is switched into operation during a different period of time in order to obtain desired performance, are meant by the "switched" controller in this context. As a matter of fact, a fuzzy logic controller behaves like a switching function in its own. As described further, the compensated response of the head possesses more-or-less equal settling time to that achieved by a PID controller, however without any overshoot. Section 2 of this paper presents the dynamic model of the head at low-frequency together with the nonlinear friction model. Section 3 presents our controller design and simulation results. Our paper also addresses the resonance problem in a micro hard drive. Since the resonance occurs in high-frequency region and can be treated in a linear manner, we present the design comparisons using a lead compensation found in standard textbooks [14-16], for instance, a complex lead-lag compensation [17], and a polynomial compensator optimized by the adaptive tabu search (ATS) [18-20]. Section 4 of the paper presents the compensation design and simulation results, while the resonance-mode model is described in the last part of section 2. Conclusion follows in section 5.

2. Dynamic Models

The dynamic of the read/write head at low-frequency is highly influenced by nonlinear characteristics and friction. To provide appropriate compensation requires accurate models of the head dynamic. Extensive theoretical and experimental studies have been conducted by Chen et. al. [21]. They reported the modelling of the read/write head as expressed by the equations (2)-(5).

$$\ddot{y} = 2.35\times10^{8}u - 6.7844\times10^{6}\arctan(0.5886y) + T_f \qquad (2)$$

$$T_f = \begin{cases} -\left[\left|1.175\times10^{6}uy + 0.01(\dot{y})^2\right| + 15000\right] \\ \quad \times \mathrm{sgn}(\dot{y}) - 282.6\dot{y}, & \dot{y}\neq 0 \\ -T_e, & \dot{y}=0, |T_e| \le T_s \\ T_s\,\mathrm{sgn}(T_e), & \dot{y}=0, |T_e| > T_s \end{cases} \qquad (3)$$

$$T_e = 2.35\times10^{8}\left[-0.02887\arctan(0.5886y) + u\right] \qquad (4)$$

$$T_s = 1.293\times10^{6}\left|u_0 y_0\right| + 1.65\times10^{4} \qquad (5)$$

where T_f = nonlinear frictional torque (Nm),
T_e = external torque (Nm),
T_s = static frictional torque (Nm),
u = input voltage (V),
u_0 = initial input voltage (V),
y = displacement of the head (m), and
y_0 = initial displacement of the head (m).

Fig. 2 illustrates various displacement curves in accordance with different input voltages fed to the VCM. These curves are obtained from the models in (2)-(5). Nonlinearities exhibit their effects quite clearly in these response curves which contain large overshoots and steady-state errors.

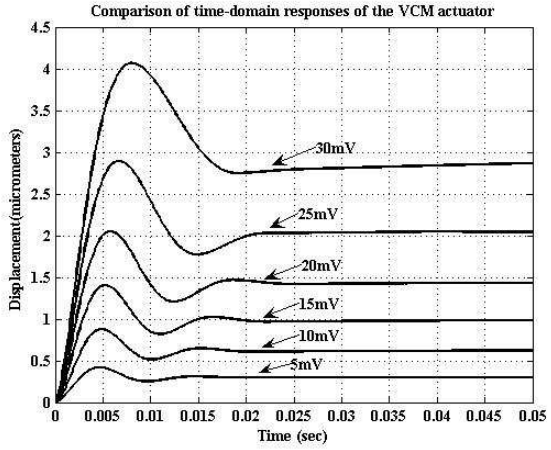

Fig. 2 Displacement curves of the read/write head corresponding to various inputs.

At high-frequency, the dynamic of a micro hard drive contains several resonance modes [21] as described by the equations (6)-(11). Fig. 3 discloses that the drive is inherently unstable.

$$G(s) = \frac{2.35\times10^{8}}{s^{2}} G_{r.m.1}(s)G_{r.m.2}(s) \times G_{r.m.3}(s)G_{r.m.4}(s)G_{r.m.5}(s) \quad (6)$$

$$G_{r.m.1}(s) = \frac{0.8709s^{2} + 1726s + 1.369\times10^{9}}{s^{2} + 1480s + 1.369\times10^{9}} \quad (7)$$

$$G_{r.m.2}(s) = \frac{0.9332s^{2} - 805.8s + 1.739\times10^{9}}{s^{2} + 125.1s + 1.739\times10^{9}} \quad (8)$$

$$G_{r.m.3}(s) = \frac{1.072s^{2} + 925.1s + 1.997\times10^{9}}{s^{2} + 536.2s + 1.997\times10^{9}} \quad (9)$$

$$G_{r.m.4}(s) = \frac{0.9594s^{2} + 98.22s + 2.514\times10^{9}}{s^{2} + 1805s + 2.514\times10^{9}} \quad (10)$$

$$G_{r.m.5}(s) = \frac{7.877\times10^{9}}{s^{2} + 6212s + 7.877\times10^{9}} \quad (11)$$

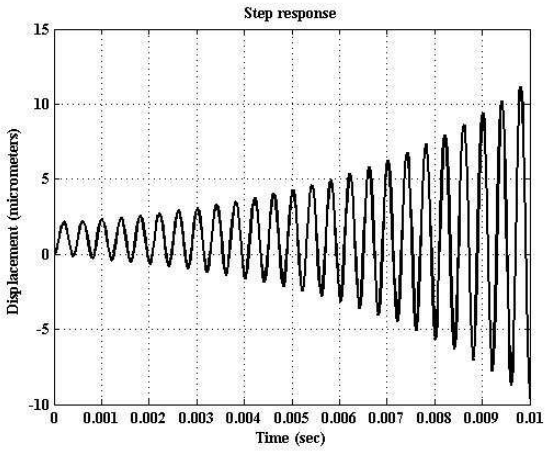

(a)

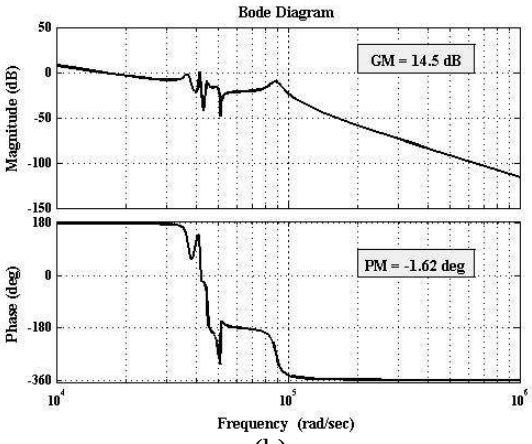

(b)

Fig. 3 (a) Time (b) frequency responses of an uncompensated micro hard drive.

3. Friction Compensation and Simulation Results

Our head control system can be represented by the block-diagram shown in Fig. 4. The proposed controller is a switched type having one set of production rules and the other of fuzzy control rules.

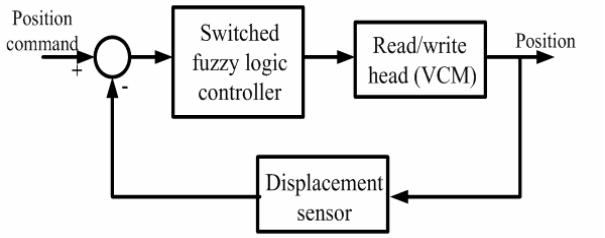

Fig. 4 Read/write head control system.

These rules are obtained heuristically based on the simulation results of the uncontrolled head. The rule-based controller is activated during the initial time t = 0 sec until time t = 1.6 msec. The controller possesses the following simple rules:

Begin: u = 0.08 V
IF (x $\geq$ 0.6 mm) THEN (u = -0.02 V)
IF (t $\geq$ 0.0015 sec AND t $\leq$ 0.0016 sec)
THEN (u = 0.01 V).

Such simple rules are effective to suppress sub-transient overshoot. The figures given in the rules are specific for 15mV-input as an example. Once the time of 1.6 msec collapses, the fuzzy logic controller is switched into action. The fuzzy controller design considers 2 inputs, and 1 output. The displacement errors (e), and the change in errors (Δe) are the inputs, while the change in control (Δu) is the output of the fuzzy control rules. Five fuzzy sets serve as the descriptions of the inputs namely negative large (NL), negative small (NS), about zero (ZE), positive small (PS), and positive large (PL), respectively. Triangular and trapezoidal membership grades are used correspondingly, and shown in Fig. 5. Six fuzzy sets of Sugeno's type are used as the descriptions of the output. These are extra largely decrease (XLD), largely decrease (LD), moderately decrease (MD), slightly decrease (SD), no change (NC), slightly increase (SI), moderately increase (MI), largely increase (LI) and extra largely increase (XLI), respectively (see Fig. 6). By the time t = 1.6 msec, the fuzzy controller is switched into action by the production rule "IF (t > 0.0016 sec) THEN ($u_{new} = u_{old} - F_{con} \times u_{old}$)". Fcon stands for the outcome obtained from the fuzzy-rule inference. Table 1 summarizes the 25 fuzzy control rules. Some of them, for instance, can be read as follows:

IF (*e is NL AND* Δ*e is NL*) *THEN* (Δ*u is XLI*)
IF (*e is NL AND* Δ*e is NS*) *THEN* (Δ*u is LI*)
⋮
IF (*e is PL AND* Δ*e is PL*) *THEN* (Δ*u is XLI*).

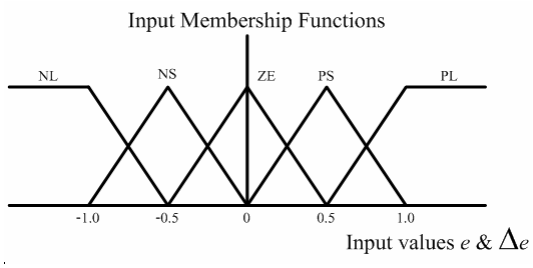

Fig. 5 Membership grades of the inputs.

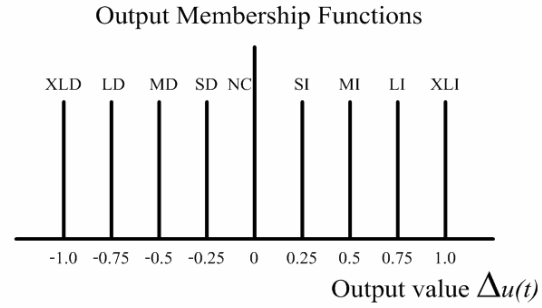

Fig. 6 Membership grades of the output.

Table1 Fuzzy control rules.

		Change in errors (Δe)				
		NL	NS	ZE	PS	PL
errors (e)	NL	XLI	LI	MI	SI	NC
	NS	LI	MI	SI	NC	SD
	ZE	MI	SI	NC	SD	MD
	PS	SI	NC	SD	MD	LD
	PL	NC	SD	MD	LD	XLI

The rule inference follows Sugeno's method [22]. At the instance of rule execution, possibly 1 up to 4 rules can be fired and Sugeno's inference provides the final outcome, F_{con}. F_{con} can be expressed as

$$F_{con} = \frac{\sum_{m=1}^{L} \Delta u_s(k_m) \times k_m}{\sum_{m=1}^{L} \Delta u_s(k_m)} \qquad (12)$$

where

Δu_s = change in control obtained from Sugeno's inference, and
k_m = singleton.

As an example, consider the following 4 rules to be fired:

1. *IF* (*e is NL AND* Δ*e is PS*) *THEN* (Δ*u is SI*)
2. *IF* (*e is NL AND* Δ*e is PL*) *THEN* (Δ*u is NC*)
3. *IF* (*e is NS AND* Δ*e is PS*) *THEN* (Δ*u is NC*)
4. *IF* (*e is NS AND* Δ*e is PL*) *THEN* (Δ*u is SD*)

Assume that the quantity e = -0.6, and Δe = 0.6, Fig. 7 illustrates the mechanisms of rule firing in accordance with the above 4 rules. Notice that the quantity e belongs to the fuzzy sets NL, and SN; Δe belongs to the sets PS, and PL, respectively. Fig. 8 and the relations (12) and (13) serve to explain the Sugeno's inference mechanism.

$$F_{con} = \frac{0.2 \times (-0.25) + 0.8 \times 0 + 0.2 \times 0.25}{0.2 + 0.8 + 0.2} = 0 \qquad (13)$$

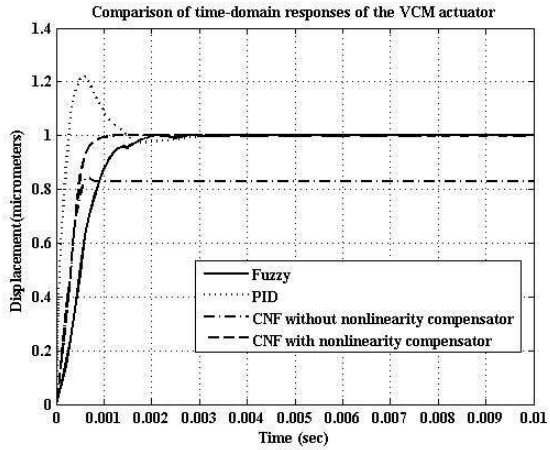

Fig. 9 Simulation results of closed-loop system.

Simulation results of the closed-loop fuzzy control system are shown in Fig. 9. For comparison purposes, the step responses under the PID control, the CNF with and without nonlinearity compensators have been taken from the reference [21]. Table 2 summarizes the settling time of each case. It can be noticed that our proposed fuzzy controller can provide a smooth response of the read/write head with zero steady-state errors, and no overshoot as also shown in Fig.10. Even though the response is not so fast as that controlled by the CNF, the structure and the design of the controller are much simpler. Moreover, the proposed controller can be

1. *IF* (*e is NL AND* Δ*e is PS*) *THEN* (Δ*u is SI*)

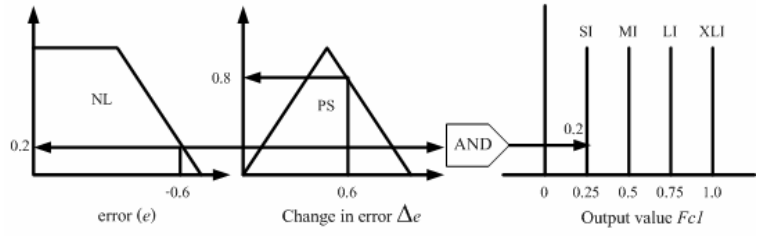

2. *IF* (*e is NL AND* Δ*e is PL*) *THEN* (Δ*u is NC*)

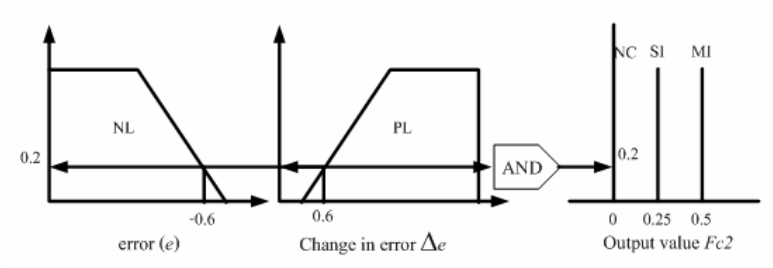

3. *IF* (*e is NS AND* Δ*e is PS*) *THEN* (Δ*u is NC*)

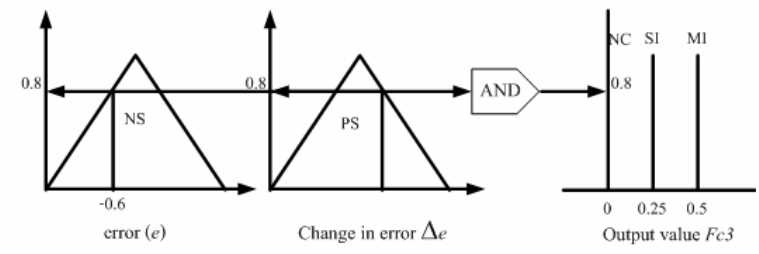

4. *IF* (*e is NS AND* Δ*e is PL*) *THEN* (Δ*u is SD*)

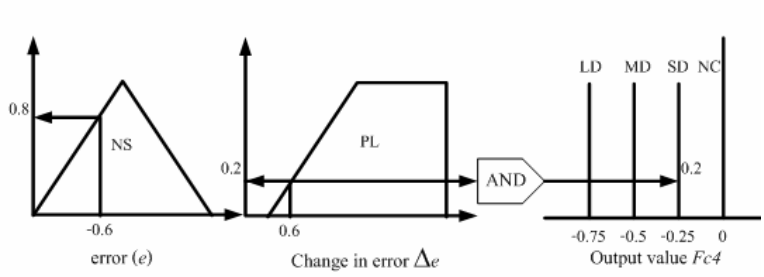

Fig. 7 Firing of fuzzy rules.

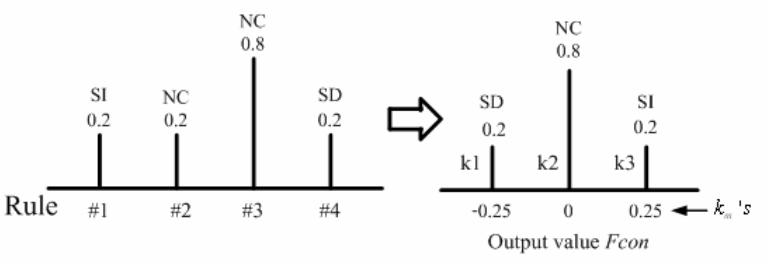

Fig. 8 Sugeno's inference.

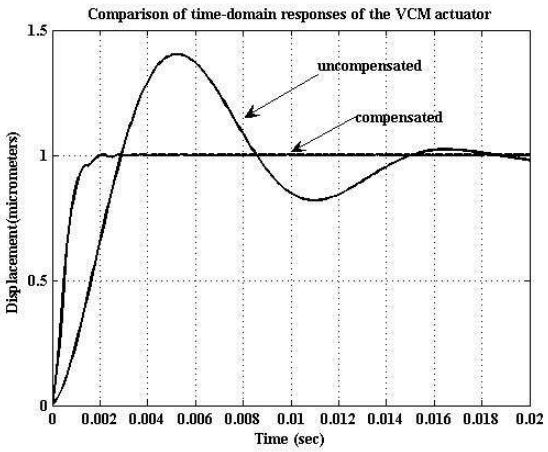

Fig. 10 Response curves of the head due to 15mV-step input.

Table 2 Settling times of each case.

Controller	PID	CNF	Fuzzy
3% settling time (msec)	1.7	0.8	1.6

modified to handle a micro-step motion control of the head. The fuzzy rules remain the same; only the production rules are modified in accordance with forward and backward directions of motion of the head. Due to the nonlinearity of the system, the rules have been heuristically modified to demonstrate this micro-stepping motion. Responses of the head with the corresponding control signals are illustrated in Figs. 11 and 12, respectively. The controlled head can move smoothly at 1 μm each step in both directions with reasonable magnitudes of the control signals. This reflects an advantage of using the proposed fuzzy controller. Moreover, a systematic optimization for this nonlinear control regime is still an open problem.

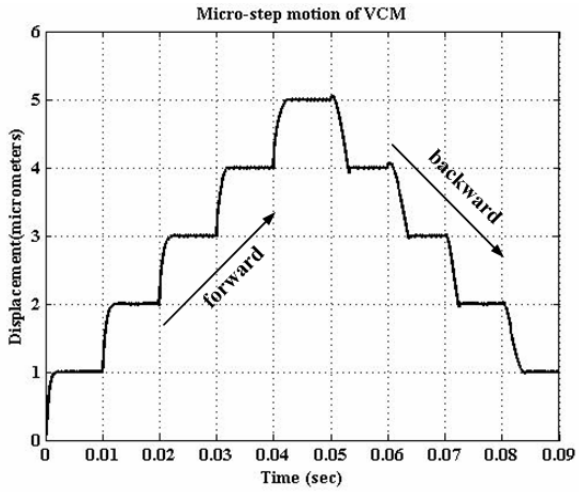

Fig. 11 Micro-step responses.

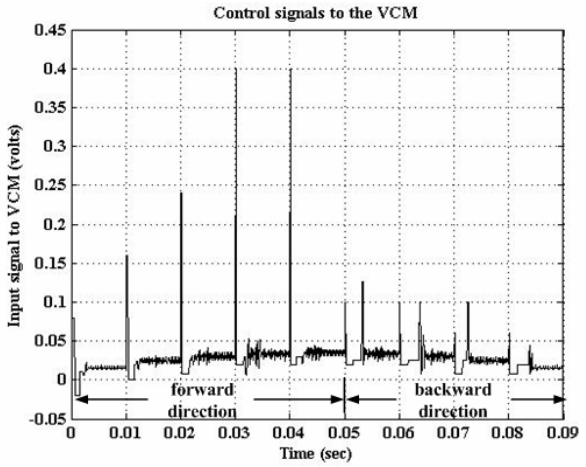

Fig. 12 Control signals of the case micro-stepping.

4. Resonance Compensation and Simulation Results

As mentioned in section 2, the high-frequency dynamic of a micro hard drive is dominated by various resonance modes that can be modeled by the transfer function in the equations (6)-(11). This paper presents some comparison studies of the resonance compensation between a cascaded lead compensator, a complex lead-lag compensator, and a polynomial compensator via search. For the cascade compensator, we apply the standard design procedures appeared in textbooks such as in [14-16]. The design method in [17] is applied to obtain the complex lead-lag compensator. The corresponding design steps are given in the appendix A. The last approach is to use search algorithm to search for a compensator of the same 4^{th}-order as the complex lead-lag one with its poles and zeros being strictly real. The search method applied is the adaptive tabu search (ATS) [18-20], whose brief description represented by a flow diagram can be found in the appendix B. The required specifications are as follows: percent overshoot ≤ 10%, settling time ≤ 10 msec, steady-state error ≤ 2%, GM ≥ 6 dB, and PM ≥ 50°. Using the conventional lead compensation approach, we have obtained the third-order compensator described by the equation (14). Fig. 13 shows the closed-loop frequency response of the compensated system having the -3dB bandwidth of 5,360 rad/sec with the corresponding GM = 9.73 dB and PM = 24.1°.

$$G_c(s) = 8.77\left(\frac{s+11578}{s+161177}\right)\left(\frac{s+60049.648}{s+453374.8449}\right) \times\left(\frac{s+13429}{s+22803}\right) \quad (14)$$

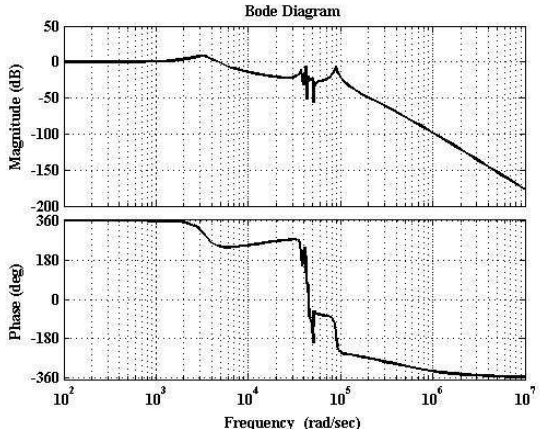

Fig. 13 Closed-loop frequency response of the compensated hard drive via a lead compensator.

The complex lead-lag method results in the compensator of 4th-order expressed as

$$G_c(s) = 2.244\left(\frac{s^2 + 3.367\times10^4 s + 3.499\times10^8}{s^2 + 1.697\times10^5 s + 8.893\times10^9}\right) \times\left(\frac{s^2 + 4636s + 8.396\times10^6}{s^2 + 1.33\times10^4 s + 5.016\times10^7}\right) \quad (15)$$

in which the following parameters are used:
1st– set: $\phi_{\max} = 45^\circ$, $\omega_m = 4.2\times10^4$ rad/sec, $\zeta = 0.9$, and
2nd–set: $\phi_{\max} = 30^\circ$, $\omega_m = 4.53\times10^3$ rad/sec, $\zeta = 0.8$.

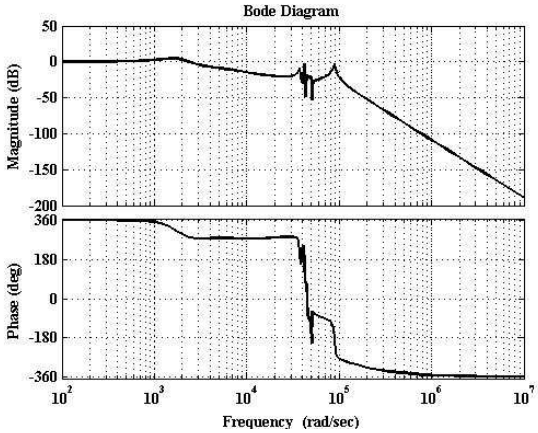

Fig. 14 Closed-loop frequency response of the compensated hard drive via a complex lead-lag compensator.

The closed-loop frequency response plot in the Fig. 14 indicates the -3dB bandwidth of 2,850 rad/sec. In addition, the corresponding GM and PM are 7.53 dB and 43.5°, respectively.

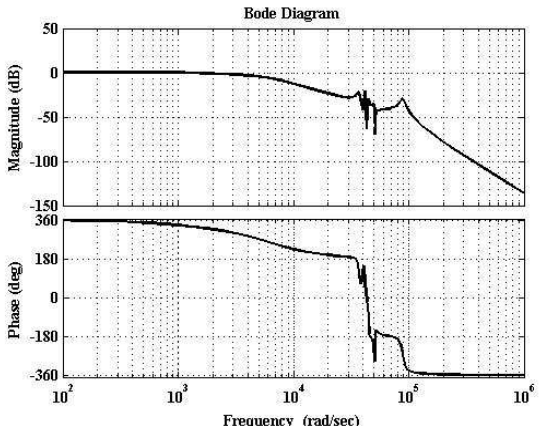

Fig. 15 Closed-loop frequency response of the compensated hard drive via a searched compensator.

The ATS has provided the compensator described by the equation (16). The following search parameters are used: search spaces for poles, zeros, and gain = [0 100,000], search radius R=10, neighborhood N = 50, termination criteria J ≤ 10 or max_iteration =100,000, allowed solution cycling = 5 before an activation of the backtracking mechanism, and 3 levels of adaptive search radius mechanism (if J ≤ 20 then R = 8, if J ≤ 15 then R = 6, and if J ≤ 12 then R = 4, respectively). The closed-loop frequency response in Fig. 15 indicates that the -3dB bandwidth = 3,780 rad/sec. In addition, the compensated system has GM = 27.1dB, and PM = 75° .

$$G_c(s) = 0.1\left(\frac{s+203.2}{s+203.2}\right)\left(\frac{s+2727}{s+4348}\right) \times\left(\frac{s+9640}{s+8920}\right)\left(\frac{s+4322}{s+6576}\right) \quad (16)$$

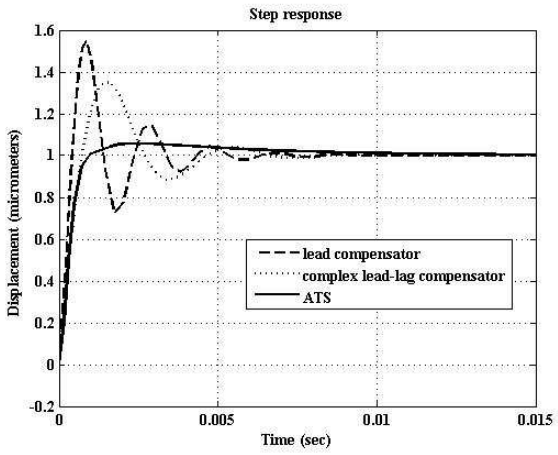

Fig. 16 Comparison of step responses.

Fig. 16 illustrates the step responses of the compensated systems for comparison purposes. The cascaded lead compensator provides the response with the shortest rise-time in an exchange of the largest overshoot. The compensator via ATS method provides the smoothest response with a moderate rise-time. The quality of the performance obtained from using the complex lead-lag compensator is in between the two. Under the consideration of ±2% steady-state error, these compensated performances settle at about the same time of 5 msec. however, the closed-loop system with the ATS-based compensator is the most robust one in terms of stability. The GMs and PMs as well as the P.O. of the responses of the systems compensated by the other two types of compensators do not meet the required specifications.

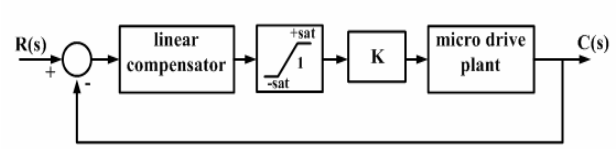

Fig. 17 Block-diagram of nonlinear compensation of a micro drive.

We attempted further to enhance the closed-loop performance of the micro-drive by incorporating gain and nonlinear element into the compensated system as represented by the diagram in Fig. 17. The linear plant is represented by the model $G(s)$ of the equation (6), while the compensator, $G_c(s)$, is of the case ATS-based method according to the equation (16). The saturation characteristic with the gain K can be viewed as a sector bounded nonlinearity depicted in Fig. 18. To apply the circle criterion [23, 24] for absolute stability consideration, it is a special case of having the slope $\alpha = 0$. Hence, the circle becomes a straight line as shown in Fig. 19. Since the gain K affects the slope of the saturation characteristic and it is bounded by the straight line of slope β, the system is always stable and the gain K can be adjusted freely as far as the Nyquist plot of the linear part dose not touch or cut the straight line show in Fig. 19. Fig. 20 shows the results of using this control approach having ± 0.9 saturation limits, K = 2, 3, and 4, respectively. With K = 2, the response settles nicely within 1 msec, and the overshoot is bounded within 10%.

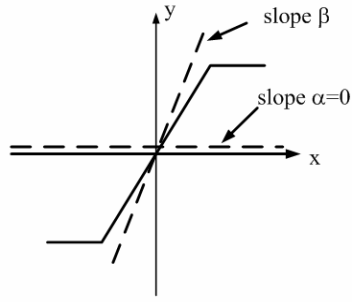

Fig. 18 Sector bounded nonlinearity.

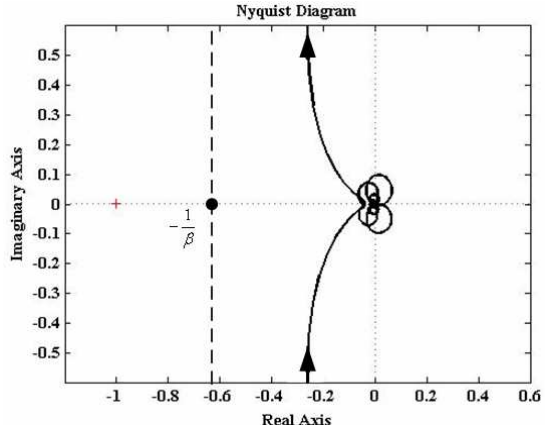

Fig. 19 Nyquist plot for the system with saturation characteristic.

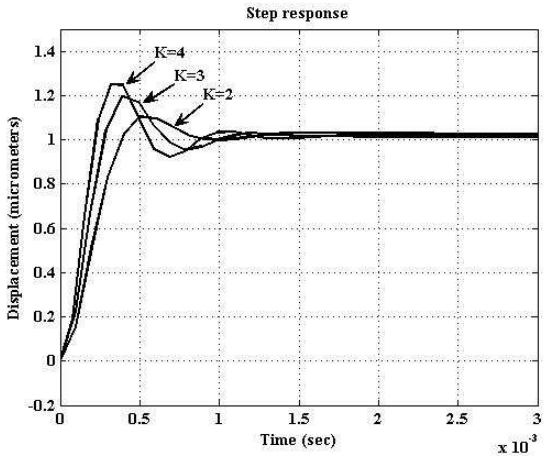

Fig. 20 Step responses of the micro hard drive having an optimized compensator with a nonlinear characteristic.

5. Conclusion

The switched-type fuzzy controller has been proposed to compensate for the nonlinear friction in a micro hard drive. The controller consists of a set of production rules, and another one of fuzzy control rules. Each rule set is switched into operation according to the dynamic response of the read/write head. The production rules come into action from the initial time t = 0 sec until 1.6 msec such that the sub-transient overshoot of the head could be suppressed. From then on, the fuzzy control rules are activated to govern the head during the rest of the transient interval up to the steady-state operation. With this arrangement, a smooth response with zero steady-state errors of the head can be achieved. The

head responds fast enough comparable to the use of a PID controller and a CNF controller. Micro-step motion control of the head is also possible through this regime as demonstrated in the paper. The production rules need a suitable design enhancement to cover the nonlinear behaviour of the micro drive. High-frequency resonance modes have been compensated for using linear control approach. Among the cascaded lead, the complex lead-lag, and the ATS-optimized polynomial compensators, the optimized compensator outperforms the rest in all aspects of performance and stability. The linearly compensated performance has been further improved by adding nonlinear saturation and gain to the control loop without sacrificing its stability. The paper demonstrates that the drive step response settles within 1 msec with its overshoot bounded by 10%.

Acknowledgements

The authors are thankful to the HDD Cluster, NECTEC, Thailand, Suranaree University of Technology (SUT), and HDD-HRD Center, SUT, for the research grants.

References

[1] L. Guo, "A new disturbance rejection scheme for hard disk drive control", *Proc. American Control Conference*, pp. 1553-1557, 1998.

[2] G. Jang, D. Kim and J.E. Oh, "New frequency domain method of nonrepeatable runout measurement in a hard disk drive spindle motor", *IEEE Trans. on Magnetics*, vol 35, pp. 833-838, 1999.

[3] T. Ohmi, "Non-repeatable runout of ball-bearing spindle-motor for 2.5″ HDD", *IEEE Trans. on Magnetic*, vol 32, pp. 1715-1720, 1996.

[4] G.F. Franklin, J.D. Powell and M. Workman, *Digital Control of Dynamical Systems (3rd. ed.)*, Addison-Wesley, 1997.

[5] B.M. Chen, T.H. Lee, K. Peng and V. Venkataramanan, "Composite nonlinear feedback control for linear systems with input saturation: theory and an application", *IEEE Trans. on Automatic Control*, vol. 43, no. 3, pp. 427-439, 2003.

[6] J-Y. Yen, F-J. Wang and Y-Y. Chen, "Fuzzy scheduling controller for a computer disk file track-following servo", *IEEE Trans. on Industrial Electronics*, vol. 40, no. 2, pp. 266-272, 1993.

[7] E.L. Branch, M. Bikdash and A. Homaifar, "Fuzzy and time-suboptimal control for dual track following and seeking drive", *Proc. 5th Biannual World Automation Congress*,Vol. 13, pp. 37-42, 2007.

[8] T. Atsumi, A Okuyama and M. Kobayashi, "Track-following control using resonant filter in hard disk drives", *IEEE/ASME Trans. on Mechatronics*, vol.12, no. 4, pp. 472-479, 2007.

[9] Y. Li, V. Venkataramanan, G. Guo and Y. Wang, "Dynamic nonlinear control for fast seek-settling performance in hard disk drives", *IEEE Trans. on Industrial Electronics*, vol. 54, no. 2, pp. 951-962, 2007.

[10] Y-M. Choi, J. Jeong and D-G. Gweon, "Modified damping scheduling proximate time optimal servomechanism for improvements in short strokes in hard disk drives", *IEEE Trans. on Magnetics*, vol. 44, no. 4, pp. 540-546, 2008.

[11] Q. Hu, C. Du, L. Xie and Y. Wang, "Discrete-time sliding mode control with time-varying surface for hard disk drives", *IEEE Trans. on Control System Technology*, vol. 17, no. 1, pp. 175-181, 2009.

[12] J. Zheng, M. Fu, Y. Wang and C. Du, "Nonlinear tracking control for a hard disk drive dual-stage actuator system", *IEEE Trans. on Mechatronics*, vol. 13, no. 5, pp. 510-518, 2008.

[13] K-S. Low and T-S. Wong, "A multiobjective genetic algorithm for optimization the performance of hard disk drive motion control system", *IEEE Trans. on Industrial Electronics*, vol. 54, n. 3, pp. 1716-1725, 2007.

[14] B.C. Kuo, *Automatic Control Systems*, Prentice-Hall, 1991.

[15] K. Ogata, *Modern Control Engineering*, Prentice-Hall, 2002.

[16] J. Dorsey, *Continuous and Discrete Control Systems*, McGraw-Hill, 2002.

[17] W.C. Messner, M.D. Bedillion, L. Xia and D.C. Karns, "Lead and lag compensators with complex poles and zeros", *IEEE Control Systems Mag*., pp. 44-54, February, 2007.

[18] D. Puangdownreong, S. Sujitjorn and T. Kulworawanichpong,"Convergence analysis of adaptive tabu search*"* *ScienceAsia*, vol. 30, no. 2, pp. 183-190, 2004.

[19] D. Puangdownreong and S. Sujitjorn,

"Image approach to system indentification", *WSEAS Trans. on Systems*, vol. 5, no. 9, pp. 930-938, 2006.

[20] J. Kluabwang, D. Puangdownreong and S. Sujitjorn, "Management agent for search algorithms with surface optimization applications", *WSEAS Trans. on Computers*, vol. 7, no. 6, pp. 791-803, 2007.

[21] B.M. Chen, T.H. Lee, K. Peng and V Venkatarmanan, *Hard Disk Drive Servo Systems*, Springer-Verlag, 2006.

[22] T. Takagi and M. Sugeno, "Fuzzy identification of system and its application to modeling and control", *IEEE Trans. on SMC*, vol.15, pp. 116-132, 1985.

[23] J-J.E. Slotine and W. Li, *Applied Nonlinear Control*, Prentice-Hall, 1991.

[24] H.K. Khalil, *Nonlinear Systems*, Pearson Education, 2000.

Appendices

A. Design steps for complex lead-lag compensation [17].

Step. 1 Choose ω_m, $\phi_{\max}$ and ζ (arbitrarily).

Step. 2 Calculate

$$\omega_p = \omega_m\left(\zeta\tan\phi_{\max} + \sqrt{\zeta^2\tan^2\phi_{\max}+1}\right)$$

$$\omega_z = \omega_m\left(-\zeta\tan\phi_{\max} + \sqrt{\zeta^2\tan^2\phi_{\max}+1}\right)$$

$$G_c(s) = \frac{\omega_p}{\omega_z}\left(\frac{s^2+2\zeta\omega_z s+\omega_z{}^2}{s^2+2\zeta\omega_p s+\omega_p{}^2}\right)$$

Step. 3 Correct the DC-gain.

B. Algorithms of the ATS.